DALTON

Properties and crystal structure of square-planar *R*,*S*,*R*,*S*-(1,3,6,8,12,15-hexaazatricyclo[13.3.1.1^{8,12}]icosane)nickel(II) perchlorate and kinetics of its isomerization to the *R*,*R*,*S*,*S* configuration†

Dongwhan Lee, Myunghyun Paik Suh* and Jae Woo Lee

Departments of Chemistry Education and Chemistry, The Center for Molecular Catalysis, Seoul National University, Seoul 151–742, Republic of Korea

The four-co-ordinate nickel(II) macrocyclic complex (*R*,*S*,*R*,*S*)-[NiL][ClO_4]$_2$, where L is 1,3,6,8,12,15-hexaazatricyclo[13.3.1.1^{8,12}]icosane, has been isolated. It shows a significantly weaker ligand field with an increased absorption coefficient and more positive electrochemical oxidation and reduction potentials compared with those of the *R*,*R*,*S*,*S* isomer. Its crystal structure was determined by X-ray crystallography. It shows a square-planar geometry with a large tetrahedral distortion of the four nitrogen donors (maximum ± 0.135 Å). The average Ni–N bond distance is 1.938(3) Å for the secondary nitrogens and 1.969(3) Å for the tertiary. The complex isomerizes to the *R*,*R*,*S*,*S* complex at 50 °C in an aqueous solution containing 9.1% (v/v) MeCN. The first-order rate constant k_{obs} is 4.16 × 10^{-5} s^{-1} at pH 7 and I = 1.0 mol dm^{-3} ($LiClO_4$). The value of k_{obs} is independent of pH and buffer concentration, but increases with increase in water content and decrease in ionic strength. The activation parameters are $\Delta H^{\ddagger}$ = 33 ± 1 kcal mol^{-1} and $\Delta S^{\ddagger}$ = 24 cal K^{-1} mol^{-1} at 25 °C. It is proposed that isomerization of the *R*,*S*,*R*,*S* to the *R*,*R*,*S*,*S* complex proceeds *via* axial co-ordination of water followed by a Ni–N(tertiary) bond dissociation assisted by a water molecule in the second co-ordination sphere acting as a general acid.

A fourteen-membered tetraaza macrocyclic complex may exist in one of five possible configurations based on the stereochemistry of the donor nitrogens.[1] Most of the known square-planar complexes of azamacrocyclic ligands have the *R*,*R*,*S*,*S* configuration which is thermodynamically the most stable. Five-co-ordinate macrocyclic complexes of Cu^{II} [2] or Ni^{II} [3] with the *R*,*S*,*R*,*S* configuration have often been prepared. However, six-[4,5] and four-co-ordinate[6–11] nickel(II) complexes having this configuration are very rare. Four-co-ordinate nickel(II) complexes with *R*,*S*,*R*,*S* configuration are known only for the macrocyclic ligands of the cyclam type (1,4,8,11-tetraazacyclotetradecane) such as *N*-methylated cyclam,[6,7] *C*-methylated cyclam,[8] a sterically congested cyclam,[9] and analogues containing fused subrings.[10,11]

Here we report the isolation, properties and crystal structure of a four-co-ordinate nickel(II) macrocyclic complex having the *R*,*S*,*R*,*S* configuration, (*R*,*S*,*R*,*S*)-[NiL][ClO_4]$_2$, where L is 1,3,6,8,12,15-hexaazatricyclo[13.3.1.1.[8,12]]icosane. We also report the kinetics of its isomerization to the *R*,*R*,*S*,*S* complex. The *R*,*S*,*R*,*S* complex shows remarkably different spectroscopic and electrochemical properties, structure and thermodynamic stability from those of the *R*,*R*,*S*,*S* isomer[12] and isomerizes to the latter irreversibly in a mixture of water and MeCN. This is the first report, to the best of our knowledge, of the kinetics and mechanism for the isomerization of a *R*,*S*,*R*,*S* nickel(II) macrocyclic complex. The configurations of the *R*,*S*,*R*,*S* and *R*,*R*,*S*,*S* isomers are shown in Scheme 1.

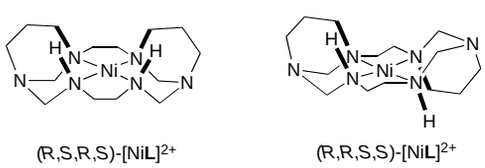

Scheme 1

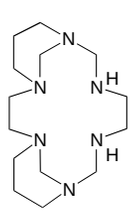

L

Experimental

Reagents

All chemicals and solvents for the synthesis were of reagent grade and used without further purification. For spectroscopic and electrochemical measurements they were purified according to the literature.[13]

Measurements

Infrared spectra were measured with a Bruker IFS48 FT-IR spectrophotometer, electronic absorption spectra with a Beckman DU68 UV/VIS spectrophotometer equipped with a temperature controller and ^{13}C NMR spectra on a Gemini-300 BB FT spectrometer. Cyclic voltammetry was carried out with a BAS 100B/W electrochemical workstation. The electrochemical data were measured in MeCN with 0.1 mol dm^{-3} $NBu^n_4PF_6$. The working electrode was a platinum disc, the auxiliary electrode a platinum wire and the reference electrode Ag–Ag$^+$ (0.01 mol dm^{-3} in MeCN).

† *Non-SI unit employed*: cal = 4.184 J.

Synthesis

CAUTION: perchlorate salts of metal complexes with organic ligands are potentially explosive. Only small amounts of material should be prepared and handled with great care.

(*R*,*S*,*R*,*S*)-[NiL][ClO$_4$]$_2$. (*a*) *Method* 1. To a Schlenk tube containing (*R*,*R*,*S*,*S*)-[NiL][ClO$_4$]$_2$·0.5H$_2$O[12] (3.0 g) and pulverized KOH (3.0 g) was slowly added MeCN (40 cm^3) which had been purified and deaerated. The mixture was stirred for 15 min under a nitrogen atmosphere during which time the yellow complex dissolved to give a deep purple solution. The solution was filtered under a nitrogen atmosphere to remove insoluble material, and distilled water (10 cm^3) was added dropwise to the filtrate. After the Ni(OH)$_2$ which formed was filtered off, the solution was concentrated by evaporation of the solvent until the orange *R*,*R*,*S*,*S* complex began to precipitate, and was filtered off. The filtrate was allowed to stand at room temperature until needle-shaped dark red crystals formed, which were filtered off, washed with MeOH, and dried *in vacuo* (yield 0.55 g, *ca*. 20%).

(*b*) *Method* 2. This method is similar to that reported previously for (*R*,*R*,*S*,*S*)-[NiL][ClO$_4$]$_2$·0.5H$_2$O[12] but modified in order to increase the yield of *R*,*S*,*R*,*S* complex by employing paraformaldehyde instead of formaldehyde, a shorter reaction time, and a different solvent system in the recrystallization procedure. To a stirred methanol solution (50 cm^3) of NiCl$_2$·6H$_2$O (11.9 g) was added *N*,*N*′-bis(3-aminopropyl)ethane-1,2-diamine (95%, 9.6 cm^3) followed by paraformaldehyde (7.5 g) and ethane-1,2-diamine (en) (3.4 cm^3). The mixture was heated at reflux for 3 h. The solution was filtered while hot, concentrated to *ca*. half its initial volume, and cooled to room temperature. A saturated methanol solution of LiClO$_4$ (13.4 g) was added to the filtrate and the solution allowed to stand in a refrigerator until an orange-red precipitate formed, which was filtered off, washed with MeOH, and dried *in vacuo* (yield 21 g, *ca*. 80%). The *R*,*S*,*R*,*S* isomer was isolated as follows. The crude product (3.4 g) was suspended in hot water (30 cm^3) and MeCN (*ca*. 15 cm^3) added dropwise with stirring until all complexes had dissolved. The solution was allowed to stand overnight at room temperature. Orange (*R*,*R*,*S*,*S*)-[NiL][ClO$_4$]$_2$·0.5H$_2$O precipitated as the major product and was filtered off. The filtrate was allowed to stand in a refrigerator until dark red crystals of the *R*,*S*,*R*,*S* complex formed, which were filtered off, washed with MeOH, and dried *in vacuo* (yield 0.30 g, *ca*. 10%) (Found: C, 31.2; H, 5.4; N, 15.55. Calc. for C$_{14}$H$_{30}$Cl$_2$NiN$_6$O$_8$: C, 31.15; H, 5.6; N, 15.55%).

X-Ray crystallography

X-Ray examination and data-collection procedures were performed at 288(2) K on a Rigaku AFC4 diffractometer. Data were collected with graphite-monochromated Mo-Kα radiation (λ 0.710 69 Å) using the ω–2θ scan technique. All data were corrected for Lorentz-polarization effects, but not for absorption. The structure was solved by direct methods using SHELXS 86.[14] Full-matrix least-squares refinement was carried out by minimizing the function $\Sigma w(F_o^2 - F_c^2)^2$. All 3814 independent data were used in the refinement. All hydrogen atoms (in calculated positions) were allowed to ride on their bonded atoms with isotropic displacement factors fixed at values 1.2 times those of the bonded atoms. All calculations were done by using the program SHELXL 93.[15] The crystallographic data collection and refinement details are summarized in Table 2.

Atomic coordinates, thermal parameters and bond lengths and angles have been deposited at the Cambridge Crystallographic Data Centre (CCDC). See Instructions for Authors, *J. Chem. Soc., Dalton Trans.*, 1997, Issue 1. Any request to the CCDC for this material should quote the full literature citation and the reference number 186/344.

Kinetic measurements

Reaction rates were measured with a Beckman DU-64 UV/VIS spectrophotometer and the temperature was controlled with a model 70 Fisher Isotemp Immersion Circulator. The pH value was measured with a model DP-880 digital pH/ion meter. Stock solutions of (*R*,*S*,*R*,*S*)-[NiL][ClO$_4$]$_2$ (3.15×10^{-2} mol dm^{-3}) and (*R*,*R*,*S*,*S*)-[NiL][ClO$_4$]$_2$·0.5H$_2$O (3.15×10^{-2} mol dm^{-3}) were made in dry MeCN since the complexes did not isomerize in MeCN in the absence of water over the temperature range 20–50 °C. Kinetic measurements were carried out in an aqueous solution containing 9.1% (v/v) MeCN except when the solvent composition was varied. Buffer solutions (0.05–0.5 mol dm^{-3}) were prepared by adding appropriate amounts of NaOH or HCl to 2-(*N*-morpholino)ethanesulfonic acid (mes) for pH 5.0–6.0, *N*′-2-(hydroxyethyl)piperazine-*N*-ethanesulfonic acid (hepes) for pH 7.0–8.0, tris(hydroxymethyl)aminomethane (tris) for pH 9.0, sodium hydrogencarbonate for pH 10.0, or sodium carbonate for pH 11.0. The ionic strength (I = 0.05–1.0 mol dm^{-3}) was adjusted with LiClO$_4$ or LiO$_3$SCF$_3$. The reactions were initiated by mixing a freshly prepared MeCN solution of (*R*,*S*,*R*,*S*)-[NiL][ClO$_4$]$_2$ (0.20 cm^3) with an aqueous solution (2.00 cm^3) of controlled pH and/or ionic strength. The concentration of the complex was 2.86×10^{-3} mol dm^{-3}. After mixing the thermostatted quartz cell was tightly closed with a tapered stopper and the reaction monitored by recording the absorbance change at 505 nm over 10 or 15 min intervals. After each kinetic run was completed the spectrum was recorded over the whole visible range (350–800 nm) and compared with that of (*R*,*R*,*S*,*S*)-[NiL][ClO$_4$]$_2$·0.5H$_2$O.

Results and Discussion

Isolation and properties of (*R*,*S*,*R*,*S*)-[NiL][ClO$_4$]$_2$

The complex (*R*,*S*,*R*,*S*)-[NiL][ClO$_4$]$_2$ was prepared by deprotonation of the secondary amines of (*R*,*R*,*S*,*S*)-[NiL][ClO$_4$]$_2$·0.5H$_2$O in MeCN followed by the addition of water. It was also isolated from the reaction product of the template condensation of *N*,*N*′-bis(3-aminopropyl)ethane-1,2-diamine, en and paraformaldehyde, similarly to (*R*,*R*,*S*,*S*)-[NiL][ClO$_4$]$_2$·0.5H$_2$O.[12] The reaction and the recrystallization procedures were modified as described in the Experimental section. The apparent colour of the *R*,*S*,*R*,*S* complex is dark red in the solid state, while that of the *R*,*R*,*S*,*S* isomer is orange.

The complex (*R*,*S*,*R*,*S*)-[NiL][ClO$_4$]$_2$ is soluble in MeCN, water and MeNO$_2$. It isomerizes quantitatively to the *R*,*R*,*S*,*S* isomer when its aqueous solution is heated at reflux for 7 h in the presence of 9.1% (v/v) MeCN, added to increase the solubility of the complex. As the solution is cooled and an excess of NaClO$_4$ is added, orange crystals of isomerized product, (*R*,*R*,*S*,*S*)-[NiL][ClO$_4$]$_2$·0.5H$_2$O, are isolated from the solution. However, the *R*,*S*,*R*,*S* complex does not isomerize in MeCN in the absence of water.

The spectroscopic properties of (*R*,*S*,*R*,*S*)-[NiL]$^{2+}$ are markedly different from those of (*R*,*R*,*S*,*S*)-[NiL]$^{2+}$ and they are compared in Table 1. The *R*,*S*,*R*,*S* complex shows maximum absorption at 489–496 nm, depending on the solvent, which is ≈20 nm to longer wavelength than that of the *R*,*R*,*S*,*S* isomer. The λ_{max} value of the *R*,*S*,*R*,*S* complex shifts to longer wavelength as the solvent is changed from MeNO$_2$ to water and MeCN. This implies that the co-ordinating solvents water and MeCN interact with the complex to some extent. Considering that *R*,*S*,*R*,*S* complexes often have a square-pyramidal geometry co-ordinating an extra axial ligand,[3] the present (*R*,*S*,*R*,*S*)-[NiL]$^{2+}$ probably co-ordinates a solvent molecule to form five-co-ordinate (*R*,*S*,*R*,*S*)-[NiL(solv)]$^{2+}$ in water or MeCN. The values of the absorption coefficient for (*R*,*S*,*R*,*S*)-[NiL][ClO$_4$]$_2$ in various solvents are greater than those of the *R*,*R*,*S*,*S* isomer. This is attributed to the increased distortions of the nickel(II) ion and nitrogen donors in the *R*,*S*,*R*,*S* complex from the ideal

Table 1 Properties of (*R*,*S*,*R*,*S*)- and (*R*,*R*,*S*,*S*)-[NiL][ClO_4]$_2$ complexes

Configuration	IR [a]/cm^{-1} ν_{NH}	UV/VIS λ_{max}/nm (ε/dm^3 mol^{-1} cm^{-1})	E_{ox} [b]/V Ni^{II}–Ni^{III}	E_{red} [b]/V Ni^{II}–Ni^{I}	^{13}C NMR,[c] δ
(*R*,*S*,*R*,*S*)	3300	489(116)[d]	+1.39	−1.01	24.7, 48.2, 48.5, 56.5, 58.2, 70.9, 74.7
	3251	490(107)[e]			
	3215	496(106)[f]			
(*R*,*R*,*S*,*S*)	3215[g]	470(88)[d]	+1.25[g]	−1.14[g]	24.3, 48.4, 49.3, 57.0, 58.2, 71.0, 74.8[g]
		472(58)[e]			
		478(36)[f]			

[a] Nujol mull. [b] In MeCN with 0.1 mol dm^{-3} $NBu^n_4ClO_4$; *vs.* SCE reference; reversible. [c] In CD_3NO_2. [d] In $MeNO_2$ at 25 °C. [e] In water at 25 °C. [f] In MeCN at 25 °C. [g] Ref. 12.

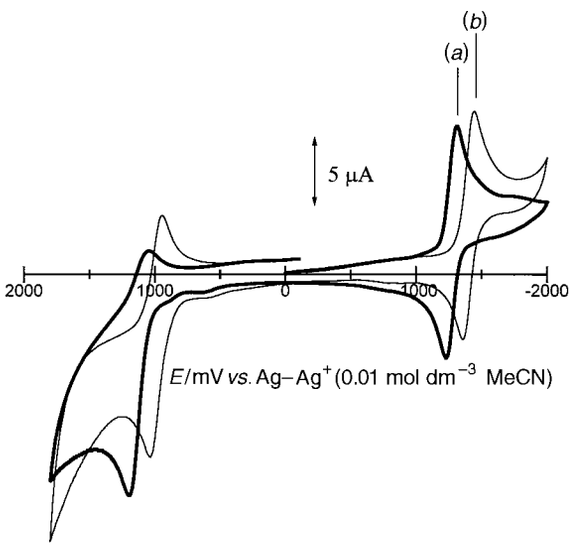

Fig. 1 Cyclic voltammograms of (*R*,*S*,*R*,*S*)-[NiL][ClO_4]$_2$ (*a*) and (*R*,*R*,*S*,*S*)-[NiL][ClO_4]$_2$·0.5H_2O (*b*) in MeCN (0.1 mol dm^{-3} $NBu^n_4PF_6$): scan rate 50 mV s^{-1}, [complex] = 2.5 mmol dm^{-3}, and 20 °C

geometry, which is revealed by the crystal structure. The value of the absorption coefficient depends on the solvent only slightly and is independent of temperature (25–75 °C) in water and MeCN, contrary to the behaviour of the *R*,*R*,*S*,*S* isomer. For the latter, the absorption coefficient is affected by the solvent: the value measured in water or MeCN is smaller than that in $MeNO_2$ and increases as the temperature increases because of an equilibrium between square-planar and octahedral species in water or MeCN.[12] Similarly to our *R*,*S*,*R*,*S* complex, some macrocyclic complexes of Ni^{II} [16] and Ag^{II} [17] with *R*,*S*,*R*,*S* configuration also absorb at longer wavelengths with greater absorption coefficients compared with those of the corresponding *R*,*R*,*S*,*S* isomers. The *R*,*S*,*R*,*S* complex usually has steric strain of the macrocycle which causes poor overlap between the metal ion and the nitrogen orbitals and results in a weaker ligand field.[10] The ^{13}C NMR spectrum of (*R*,*S*,*R*,*S*)-[NiL][ClO_4]$_2$ is slightly different from that of the *R*,*R*,*S*,*S* isomer (Table 1).

The *R*,*S*,*R*,*S* complex decomposes by losing the metal ion in acidic aqueous solution (pH ⩽ 6.0) at 50 °C while the *R*,*R*,*S*,*S* isomer is stable at room temperature in 0.1 mol dm^{-3} $HClO_4$.[12] At pH 5.0 ([mes] = 0.05 mol dm^{-3}), 50 °C and *I* = 0.1 mol dm^{-3} (NaCl) the two isomers decompose at different rates. The first-order rate constant for decomposition of the *R*,*S*,*R*,*S* complex is (6.32 ± 0.03) × 10^{-5} s^{-1}, which is *ca.* 3 times greater than the (2.23 ± 0.02) × 10^{-5} s^{-1} of the *R*,*R*,*S*,*S* complex. Dissociation of metal ions from fourteen-membered macrocyclic complexes in acidic media often accompanies isomerization of the macrocycle.[18] The present complex, however, does not isomerize under the experimental conditions, as is ascertained by the absorbance change which occurs without shift in λ_{max} during the decomposition process. The *R*,*S*,*R*,*S* complex is also unstable in basic solution and decomposes at pH ⩾ 10 with the formation of $Ni(OH)_2$.

Table 2 Crystal data and data collection details for (*R*,*S*,*R*,*S*)-[NiL][ClO_4]$_2$

Formula	$C_{14}H_{30}Cl_2N_6NiO_8$
M	540.05
Crystal system	Monoclinic
Space group	$P2_1/n$
a/Å	7.883(2)
b/Å	14.361(5)
c/Å	19.139(5)
β/°	93.10(3)
U/Å^3	2163.4(10)
Z	4
D_c/g cm^{-3}	1.658
Crystal size/mm	0.60 × 0.40 × 0.25
μ/cm^{-1}	11.99
No. data collected	4114
No. independent reflections (all)	3814 (R_{int} = 0.0312)
No. observed data [$F > 4\sigma(F)$]	2755
No. variable parameters	281
F(000)	1128
$R(F)$[a] (all data)	0.0863
$wR(F^2)$[b] (all data)	0.1588
Goodness of fit (all data)	1.079

[a] $R = \Sigma\ ||F_o| - |F_c||/\Sigma|F_o|$. [b] $wR(F^2) = [\Sigma w(F_o^2 - F_c^2)^2/\Sigma w(F_o^2)^2]^{\frac{1}{2}}$, $w = 1/[\sigma^2(F_o)^2 + (0.0564P)^2 + 7.6666P]$ where $P = (F_o^2 + 2F_c^2)/3$.

The cyclic voltammograms of the *R*,*S*,*R*,*S* and *R*,*R*,*S*,*S* complexes are presented in Fig. 1 and the data are summarized in Table 1. The electrochemical properties of (*R*,*S*,*R*,*S*)-$[NiL]^{2+}$ are markedly different from those of (*R*,*R*,*S*,*S*)-$[NiL]^{2+}$ although the two isomers differ only in the relative position of the subring moieties in the macrocycle. The *R*,*S*,*R*,*S* isomer shows a reversible one-electron oxidation at +1.39 V and a reversible one-electron reduction at −1.01 V *vs.* saturated calomel electrode (SCE). Compared with the *R*,*R*,*S*,*S* complex, they are shifted by +0.14 and +0.13 V, respectively. The anodic shifts in the oxidation and reduction potentials were also observed with the *R*,*S*,*R*,*S*-nickel(II) complexes of cyclam derivatives.[9,19] These anodic shifts of the redox potentials may be related to the reduced ligand-field strength of the *R*,*S*,*R*,*S* complex which stabilizes the antibonding σ orbitals and makes addition of an electron more favourable while removal of an electron is less favourable.[20]

Crystal structure of (*R*,*S*,*R*,*S*)-[NiL][ClO_4]$_2$

An ORTEP[21] view of the cation for (*R*,*S*,*R*,*S*)-[NiL][ClO_4]$_2$ is presented in Fig. 2. Table 3 shows selected bond distances and angles. The geometry around the Ni^{II} approximates to square planar, involving two secondary and two tertiary amine nitrogens of the macrocycle. The closest axial contacts of the Ni^{II} with the oxygen atoms of the perchlorate anions are 2.942(5) and 3.325(5) Å. However, there is a large tetrahedral distortion of the four nitrogen donors; N(3) and N(10) lie below the least-squares co-ordination plane by 0.135(3) and 0.129(3) Å,

Table 3 Bond distances (Å) and angles (°) for (*R*,*S*,*R*,*S*)-[NiL][ClO_4]$_2$

Ni–N(6)	1.937(4)	C(4)–C(5)	1.453(9)	C(11)–C(12)	1.394(11)	C(15)–C(16)	1.498(11)
Ni–N(3)	1.939(4)	C(5)–N(6)	1.490(7)	C(12)–N(13)	1.500(9)	C(16)–C(17)	1.531(11)
Ni–N(13)	1.964(5)	N(6)–C(7)	1.500(8)	N(13)–C(15)	1.477(8)	C(18)–C(19)	1.495(10)
Ni–N(10)	1.974(5)	C(7)–N(8)	1.419(8)	N(13)–C(14)	1.509(8)	C(19)–C(20)	1.489(11)
N(1)–C(14)	1.420(8)	N(8)–C(9)	1.437(8)	Cl(1)–O(13)	1.403(6)	Cl(2)–O(24)	1.419(5)
N(1)–C(2)	1.436(8)	N(8)–C(18)	1.459(8)	Cl(1)–O(12)	1.416(5)	Cl(2)–O(23)	1.432(5)
N(1)–C(17)	1.471(9)	C(9)–N(10)	1.510(8)	Cl(1)–O(14)	1.430(5)	Cl(2)–O(21)	1.434(5)
C(2)–N(3)	1.492(7)	N(10)–C(11)	1.505(9)	Cl(1)–O(11)	1.435(5)	Cl(2)–O(22)	1.439(5)
N(3)–C(4)	1.493(7)	N(10)–C(20)	1.515(9)				
N(6)–Ni–N(3)	85.4(2)	C(4)–C(5)–N(6)	107.6(5)	C(20)–N(10)–Ni	117.7(4)	C(14)–N(13)–Ni	109.9(4)
N(6)–Ni–N(13)	168.0(2)	C(5)–N(6)–C(7)	107.6(5)	C(12)–C(11)–N(10)	110.0(6)	N(1)–C(14)–N(13)	112.0(5)
N(3)–Ni–N(13)	93.7(2)	C(5)–N(6)–Ni	108.2(3)	C(11)–C(12)–N(13)	113.1(7)	N(13)–C(15)–C(16)	113.8(6)
N(6)–Ni–N(10)	93.5(2)	C(7)–N(6)–Ni	117.0(4)	C(15)–N(13)–C(12)	111.1(6)	C(15)–C(16)–C(17)	111.3(6)
N(3)–Ni–N(10)	176.1(2)	N(8)–C(7)–N(6)	115.8(5)	C(15)–N(13)–C(14)	106.7(5)	N(1)–C(17)–C(16)	112.8(5)
N(13)–Ni–N(10)	88.2(2)	C(7)–N(8)–C(9)	112.7(5)	C(12)–N(13)–C(14)	105.9(6)	N(8)–C(18)–C(19)	113.3(5)
C(14)–N(1)–C(2)	114.1(5)	C(7)–N(8)–C(18)	116.5(6)	C(15)–N(13)–NI	119.8(4)	C(20)–C(19)–C(18)	111.3(7)
C(14)–N(1)–C(17)	110.7(6)	C(9)–N(8)–C(18)	112.7(5)	C(12)–N(13)–NI	102.6(4)	C(19)–C(20)–N(10)	114.8(5)
C(2)–N(1)–C(17)	117.1(6)	N(8)–C(9)–N(10)	111.9(5)	O(13)–Cl(1)–O(12)	108.9(5)	O(24)–Cl(2)–O(23)	110.1(3)
N(1)–C(2)–N(3)	115.2(5)	C(11)–N(10)–C(9)	110.8(6)	O(13)–Cl(1)–O(14)	110.1(4)	O(24)–Cl(2)–O(21)	111.2(4)
C(2)–N(3)–C(4)	112.3(5)	C(11)–N(10)–C(20)	105.2(6)	O(12)–Cl(1)–O(14)	108.5(4)	O(23)–Cl(2)–O(21)	108.6(3)
C(2)–N(3)–Ni	115.7(4)	C(9)–N(10)–C(20)	106.7(5)	O(13)–Cl(1)–O(11)	109.7(4)	O(24)–Cl(2)–O(22)	110.1(3)
C(4)–N(3)–Ni	110.7(3)	C(11)–N(10)–Ni	107.2(4)	O(12)–Cl(1)–O(11)	109.6(4)	O(23)–Cl(2)–O(22)	108.2(3)
C(5)–C(4)–N(3)	108.1(5)	C(9)–N(10)–Ni	109.2(4)	O(14)–Cl(1)–O(11)	110.1(3)	O(21)–Cl(2)–O(22)	108.5(3)

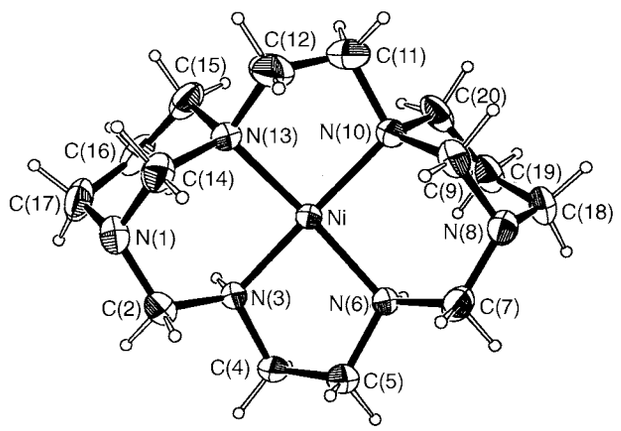

Fig. 2 An ORTEP view of the cation in (*R*,*S*,*R*,*S*)-[NiL][ClO_4]$_2$ showing the atomic labelling scheme. The atoms are represented by 30% probability thermal ellipsoids

respectively, while N(6) and N(13) lie above the plane by 0.135(3) and 0.130(3) Å, respectively. The bond angles N(6)–Ni–N(13) and N(3)–Ni–N(10) are 168.0(2) and 176.1(2)°, respectively. The Ni^{II} is displaced 0.071 Å out of the co-ordination plane toward the subring moieties. The distortions of the nitrogen donors and Ni^{II} from ideal geometry are significantly increased compared with those of the *R*,*R*,*S*,*S* isomer in which the nitrogen donors deviate by *ca*. 0.020 Å and the Ni^{II} is 0.02 Å out of the square plane.[12] These increased distortions result in the increased absorption coefficient of the *R*,*S*,*R*,*S* complex compared with that of the *R*,*R*,*S*,*S* isomer. The complex contains two 1,3-diazacyclohexane subrings which are fused to amino functions at the bridgehead position and disposed at the same side with respect to the co-ordination plane together with the two secondary amine hydrogens. The two subrings have chair conformations.

The Ni–N bond distances range from 1.937(4) to 1.974(5) Å. Those involving tertiary nitrogen donors [1.969(3) Å (average)] are significantly longer than those [1.938(3) Å (average)] involving secondary nitrogen donors. In the *R*,*R*,*S*,*S* isomer also, a similar difference exists; 1.961(1) (average) and 1.942(1) Å (average).[12] In general, tertiary nitrogens bind Ni^{II} less strongly than secondary nitrogens and the corresponding Ni–N bonds are often longer.[12,19,22] Since the *R*,*S*,*R*,*S* complex has a weaker ligand field than the *R*,*R*,*S*,*S* isomer, the former is expected to have longer Ni–N bond distances than the latter. However, the average Ni–N bond distance [1.950(2) Å] of the *R*,*S*,*R*,*S* complex is nearly identical to that [1.951(2) Å] of the *R*,*R*,*S*,*S* complex.

The six- and five-membered chelate rings assume a chair and an asymmetric *gauche* conformation, respectively. The bite angles of the five-membered chelate rings are 88.2(2) and 85.4(2)° and those of the six-membered chelate rings 93.7(2) and 93.5(2)°. The bite distances of the five-membered chelate rings are 2.628(6) and 2.740(7) Å and those of the six-membered chelate rings 2.849(7) and 2.847(7) Å, respectively. Especially the C–C bonds of the ethane-1,2-diamine moieties in the five-membered chelate rings having the asymmetric *gauche* conformation are abnormally short: C(4)–C(5) and C(11)–C(12) are 1.453(9) and 1.394(11) Å, respectively. This indicates that a significant strain exists in the five-membered chelate rings.

The C–N bond distances [1.439(3) Å (average)] involving unco-ordinated bridgehead tertiary amines N(1) and N(8), ranging from 1.419(8) to 1.471(9) Å, are shorter than normal aliphatic C–N bond distances (1.52 Å). The bond angles involving N(1) and N(8) are 111–117°. Similar shortening of the C–N bond distances as well as the flattening of the bond angles involving the bridgehead tertiary nitrogen has been observed for (*R*,*R*,*S*,*S*)-[NiL][ClO_4]$_2$·0.5H_2O[12] and other polyaza macrocyclic complexes,[23] and is attributed to the partial contribution of sp^2 hybridization of the bridgehead nitrogens.

Isomerization of (*R*,*S*,*R*,*S*)- to (*R*,*R*,*S*,*S*)-[NiL]$^{2+}$

Although the *R*,*S*,*R*,*S* complex does not isomerize in MeCN, it does in the presence of water. Fig. 3 shows the spectral change of the *R*,*S*,*R*,*S* complex in an aqueous solution containing 9.1% (v/v) MeCN, at 50 °C, pH 7.0 ([hepes] = 0.05 mol dm^{-3}) and I = 0.1 mol dm^{-3} ($LiClO_4$). The final spectrum of the *R*,*S*,*R*,*S* complex shows a maximum at 473 nm, identical to that of (*R*,*R*,*S*,*S*)-[NiL][ClO_4]$_2$·0.5H_2O.[12] The spectral change caused by the temperature decrease from 50 to 25 °C in Fig. 3 is attributed to an equilibrium between the square-planar and octahedral species of the resulting *R*,*R*,*S*,*S* complex in the solvent system used. The latter complex co-ordinates donor solvent molecules to form high-spin octahedral species and the amount of the octahedral species increases as the temperature is lowered,[12] which results in the absorbance decrease at 473 nm. Fig. 4

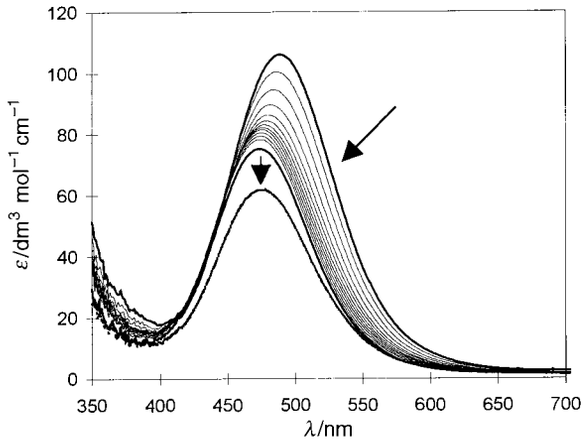

Fig. 3 Spectral changes of (*R*,*S*,*R*,*S*)-[NiL][ClO_4]$_2$ at 50 °C in an aqueous solution containing 9.1% (v/v) MeCN, at pH 7.0 ([hepes] = 0.05 mol dm^{-3}) and I = 0.1 mol dm^{-3} ($LiClO_4$). Spectra were recorded every 2 h and the final spectrum 30 h after the start. The vertical arrow represents the final spectrum measured at 25 °C

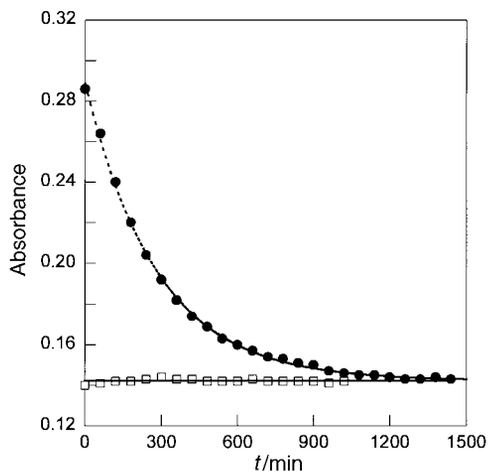

Fig. 4 Absorbance changes of (*R*,*S*,*R*,*S*)- (●) and (*R*,*R*,*S*,*S*)-[NiL][ClO_4]$_2$ (□) at 505 nm in an aqueous solution containing 9.1% (v/v) MeCN: [complex] = 2.86 mmol dm^{-3}, 50 °C, I = 0.1 mol dm^{-3} (KCl). Dashed line is the best-fit curve for the pseudo-first-order reaction with k_{obs} = (5.90 ± 0.09) × 10^{-5} s^{-1}

shows the absorbance changes of the two isomers measured at 505 nm in an aqueous solution containing 9.1% (v/v) MeCN at 50 °C. The absorbance of the *R*,*S*,*R*,*S* complex decreases and eventually becomes identical to that of the *R*,*R*,*S*,*S* complex. The first-order rate constant for the isomerization is (5.90 ± 0.09) × 10^{-5} s^{-1}. However, the *R*,*R*,*S*,*S* complex does not change its absorbance under the same conditions, showing that it does not isomerize.

In the *R*,*S*,*R*,*S* complex the strained asymmetric *gauche* conformation of the five-membered chelate rings and the non-bonded interaction between the two subrings located in the same direction of the macrocyclic plane make the complex less stable than the *R*,*R*,*S*,*S* isomer and the *R*,*S*,*R*,*S* complex isomerizes to the thermodynamically more stable *R*,*R*,*S*,*S* complex. The greater ligand-field stabilization energy and the better affinity for the axial co-ordination of a solvent molecule by the *R*,*R*,*S*,*S* complex also may be the driving force for the thermal isomerization.[18c]

Kinetics of isomerization

The rate of isomerization from the *R*,*S*,*R*,*S* to the *R*,*R*,*S*,*S* complex was measured from the absorbance change of (*R*,*S*,*R*,*S*)-$[NiL]^{2+}$ at 505 nm where the difference in the absorptivities of the two isomers is maximal. Good first-order kinetics

Table 4 pH-Dependent k_{obs} values[a] for the isomerization of *R*,*S*,*R*,*S*- to *R*,*R*,*S*,*S*-$[NiL]^{2+}$

pH	$10^5 k_{obs}/s^{-1}$
6.0	—[b]
7.0	5.75 ± 0.10
8.0	5.94 ± 0.03
9.0	5.26 ± 0.03
10.0	—[c]

[a] Measured in aqueous solution containing 9.1% (v/v) MeCN at 50 °C, I = 0.1 mol dm^{-3} (NaCl), and buffer concentration of 0.05 mol dm^{-3}. [b] Reaction rate could not be measured because of decomposition of the complex at pH ≤ 6. [c] Reaction rate could not be measured at pH ≥ 10 because of demetallation of the complex through formation of $Ni(OH)_2$.

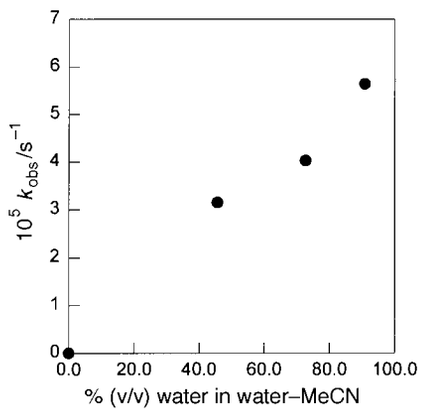

Fig. 5 Relationship between k_{obs} and the volume fraction of water in the water–MeCN mixture at 50 °C and I = 0.1 mol dm^{-3} ($LiClO_4$)

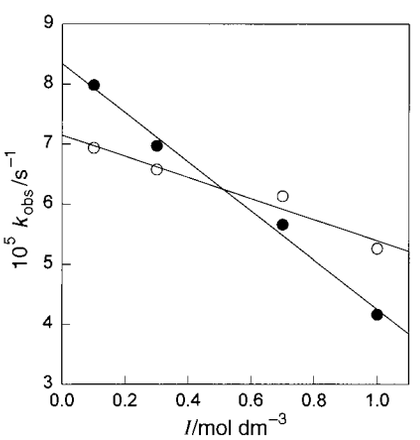

Fig. 6 Relationship between k_{obs} and ionic strength (I) in an aqueous solution containing 9.1% (v/v) MeCN at 50 °C and pH 7.0 ([hepes] = 0.05 mol dm^{-3}): (●) $LiClO_4$, (○) LiO_3SCF_3

were observed in all cases. The values of the first-order rate constant (k_{obs}) were measured at various pH, fraction of water in the mixed solvent system of water–MeCN, ionic strength, buffer concentration and temperature.

The pH dependence of k_{obs} is summarized in Table 4. The ionic strength was controlled with NaCl since either HCl or NaOH was used to adjust the pH of the buffer solution. Kinetic measurements were possible only at pH 7–9 because *R*,*S*,*R*,*S*-$[NiL]^{2+}$ decomposed gradually at pH ≤ 6.0 and was instantaneously demetallated at pH ≥ 10 as previously mentioned. The value of k_{obs} is nearly insensitive to change in pH at pH 7–9. On the other hand, it strongly depends on the solvent composition and ionic strength of the solution, as shown in Figs. 5 and 6. The effect of the solvent composition (Fig. 5) was measured without adjustment of pH because of (*i*) the pH values for

the mixed-solvent system have little meaning, especially when the volume fraction of the organic solvent is high and (*ii*) the pH value of the aqueous solution hardly affects the k_{obs} value as shown in Table 4. In the aprotic polar solvent MeCN the complex did not isomerize. However, it isomerized with increased rate as the fraction of water increased [45–91% (v/v)] in water–MeCN media (Fig. 5). When the volume fraction of water was less than 45% the rate of isomerization was too slow to be measured. The value of k_{obs} increases almost linearly as the volume fraction of water increases, but the molecularity of water participating in the transition state would not necessarily be one if the solvent effect of water is taken into account.

The value of k_{obs} at 50 °C varies almost negligibly upon change of the buffer (hepes) concentration: at pH 7.0 and $I = 1.0$ mol dm^{-3} ($LiClO_4$), the values of k_{obs} were (4.16 ± 0.03) × 10^{-5} s^{-1} at [hepes] = 0.05 mol dm^{-3} and (4.28 ± 0.02) × 10^{-5} s^{-1} at [hepes] = 0.5 mol dm^{-3}. However, as the ionic strength of the solution was increased from 0.1 to 1.0 mol dm^{-3} by using $LiClO_4$ or LiO_3SCF_3 at pH 7.0 (Fig. 6), the value of k_{obs} decreased by 20–50% and varied almost linearly as I increased. It is noteworthy that the nature of the electrolyte slightly affects the rate of isomerization. Co-ordination of an axial ligand to the square-planar complex has been shown to affect the rate constant for configurational change of a macrocyclic ligand.[24] In this respect, it might be suspected that the Cl^- ion adopted in Fig. 4 and Table 4 to adjust the ionic strength can affect the k_{obs} values since it is a potential axial ligand. The values of k_{obs} at 50 °C are (5.90 ± 0.09) × 10^{-5} and (5.64 ± 0.05) × 10^{-5} s^{-1} at 0.1 mol dm^{-3} KCl and 0.1 mol dm^{-3} $LiClO_4$, respectively (Figs. 4 and 5), without adjustment of pH in an aqueous solution containing 9.1% (v/v) MeCN. The k_{obs} value is (5.75 ± 0.10) × 10^{-5} s^{-1} at 0.1 mol dm^{-3} NaCl and pH 7 (Table 4). Therefore, it is evident that the axial binding of Cl^- ion does not occur in this solvent system and this ion is kinetically innocent.

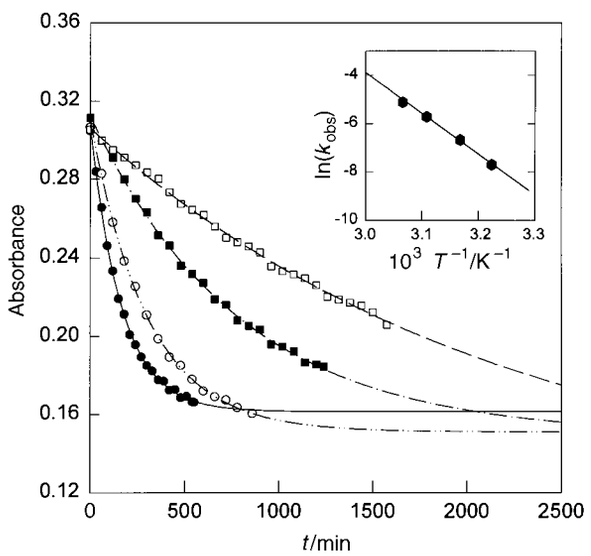

Fig. 7 Temperature dependence of the absorbance change for (*R*,*S*,*R*,*S*)-[NiL][ClO_4]$_2$ in an aqueous solution containing 9.1% (v/v) MeCN at 505 nm, pH 7.0 ([hepes] = 0.05 mol dm^{-3}), $I = 0.1$ mol dm^{-3} ($LiClO_4$): 326 (●), 321 (○), 315 (■) and 310 K (□). Inset: Arrhenius plot

The values of k_{obs} were measured at various temperatures in the range 310–326 K (Fig. 7) and the kinetic parameters E_a 33.5 ± 0.2 kcal mol^{-1}, $\Delta H^{\ddagger} = 33 \pm 1$ kcal mol^{-1} and $\Delta S^{\ddagger} = 24$ cal K^{-1} mol^{-1} at 25 °C were estimated from an Arrhenius plot.

The kinetic results are summarized as follows: (*i*) the rate law is $-d[(R,S,R,S)\text{-}Ni^{II}L]/dt = k_{obs}[(R,S,R,S)\text{-}Ni^{II}L]$, (*ii*) k_{obs} increases as the content of water increases, (*iii*) k_{obs} is independent of pH at pH 7.0–9.0, (*iv*) k_{obs} is not affected by the buffer concentration (hepes) at pH 7.0 and $I = 1.0$ mol dm^{-3} ($LiClO_4$), (*v*) k_{obs} decreases as the ionic strength of the solution increases and (*vi*) the activation parameters are $\Delta H^{\ddagger} = 33 \pm 1$ kcal mol^{-1} and $\Delta S^{\ddagger} = 24$ cal K^{-1} mol^{-1} at 25 °C.

Isomerization mechanism

In order to change the configuration of the macrocycle from (*R*,*S*,*R*,*S*)- to (*R*,*R*,*S*,*S*)-[NiL]$^{2+}$ inversion of one tertiary and one secondary nitrogen in a six-membered chelate ring should occur. A mechanism which accommodates the kinetic results is shown in Scheme 2.

To initiate the configurational change a Ni–N bond should be dissociated. This will occur at the tertiary amine sites instead of the secondary as is supported by the following arguments: (*i*) tertiary Ni–N bonds [1.969(3) Å (average)] are longer than secondary ones [1.938(3) Å (average)]; (*ii*) the methylenediamene units contained in the macrocycle are unstable unless their nitrogens are tertiary[25] or directly co-ordinated.[12,26,27] There-

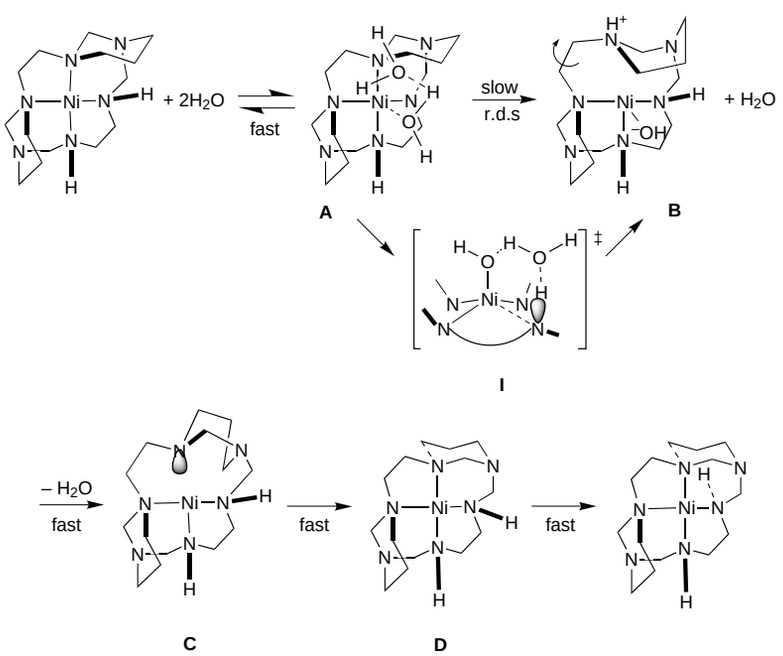

Scheme 2

fore, the methylenediamine linkages are stable even after dissociation from the metal ion only if a tertiary nitrogen donor is dissociated rather than a secondary. In case of the macrocyclic system, angular expansion of a M–N bond is necessary for chelate-ring opening and will be facilitated by protonation of the leaving nitrogen[28] since the solvation pathway[18a] is not accessible because solvent co-ordination at the dissociated site is sterically hindered by the macrocycle to a large extent. Based on the experimental results that the k_{obs} values are insensitive to pH and buffer concentration but strongly depend on the water fraction in water–MeCN media, it can be suggested that water acts as a proton donor in the Ni–N bond dissociation.

Prior to the rate-determining step (r.d.s.) there exists an equilibrium between square-planar (*R*,*S*,*R*,*S*)-$[NiL]^{2+}$ and five-co-ordinate (*R*,*S*,*R*,*S*)-$[NiL(H_2O)]^{2+}$ species.[3] In the latter a water molecule is co-ordinated at the axial site of $[NiL]^{2+}$ in the same direction as the two subrings of the macrocycle because the Ni^{II} in (*R*,*S*,*R*,*S*)-$[NiL]^{2+}$ lies out of the co-ordination plane (0.071 Å) toward the subrings. In the transition state **I** the leaving nitrogen is protonated by a H_2O molecule of the second co-ordination sphere which is hydrogen bonded to the co-ordinated axial H_2O to increase its acidity,[29] and is dissociated from the metal ion. For geometric reasons, the co-ordinated axial H_2O cannot act as a proton donor. A similar protonation pathway involving general acid catalysis has been proposed for the dissociation of metal–amine or –amide nitrogen bonds.[30]

The fact that value of k_{obs} decreases as the ionic strength of the media increases can be explained by the formation of the less polarized intermediate **I** the charge on which is delocalized by co-ordination of OH^- to Ni^{II} and protonation at the leaving nitrogen. It may be also related with the formation of a reduced amount of the five-co-ordinate species (*R*,*S*,*R*,*S*)-$[NiL(H_2O)]^{2+}$ as the ionic strength increases, similarly to the case of the *R*,*R*,*S*,*S* isomer which provides less octahedral species in water as the ionic strength increases.[12] As previously stated, the k_{obs} values are nearly insensitive to the nature of the electrolyte such as NaCl, KCl and $LiClO_4$, and the dependence of k_{obs}/I (Fig. 6) on the type of electrolyte used ($LiClO_4$ *vs.* LiO_3SCF_3) cannot be clearly understood at this stage. The positive value of $\Delta S^{\ddagger}$ (24 cal K^{-1} mol^{-1}) may be attributed to the increased entropy caused by the bond dissociation and ring flipping as well as the liberation of one water molecule in the transition state, although it would be also affected by the overall alteration of the solvent structure.

Although the details of the fast steps following the rate-determining step cannot be verified, at least two different stages involving the *R*,*R*,*R*,*S* configuration[31–34] **D** may exist in order to complete the configurational change to the *R*,*R*,*S*,*S* complex.

The reverse isomerization from the *R*,*R*,*S*,*S* to the *R*,*S*,*R*,*S* configuration is also of interest since the former complex is thermodynamically the more stable. It has been previously reported that a co-ordinating solvent,[31] extra ligand,[35] and pendant donor group[5] induced this process.

Conclusion

The square-planar nickel(II) complex (*R*,*S*,*R*,*S*)-$[NiL][ClO_4]_2$ exhibits significantly different spectroscopic, eletrochemical, and structural properties to those of the *R*,*R*,*S*,*S* isomer. The former complex has a weaker ligand field and increased molar absorption and anodic shifts in the electrochemical oxidation and reduction potentials due to the poor overlap of Ni^{II} and nitrogen orbitals. Although it does not isomerize in MeCN, it does in the presence of water. The rate of isomerization increases as the water content increases and decreases as the ionic strength increases. The kinetic study of the isomerization revealed that the configurational change of the macrocycle is driven by co-ordination of water followed by a Ni–N bond dissociation assisted by a water molecule in the second co-ordination sphere acting as a general acid.

Acknowledgements

This work was supported by the Basic Research Program (BSRI 95-3415), Ministry of Education and the Center for Molecular Catalysis, Korean Science and Engineering Foundation.

References

1 B. Bosnich, C. K. Poon and M. L. Tobe, *Inorg. Chem.*, 1965, **4**, 1102.
2 T.-J. Lee, T.-Y. Lee, C.-Y. Hong, D.-T. Wu and C.-S. Chung, *Acta Crystallogr., Sect. C*, 1986, **42**, 999; T.-H. Lu, W.-C. Liang, D.-T. Wu and C.-S. Chung, *Acta Crystallogr., Sect. C*, 1986, **42**, 801; T.-H. Lu, D.-T. Wu and C.-S. Chung, *J. Chem. Soc., Dalton Trans.*, 1986, 1999; D. Tschudin, A. Riesen and T. A. Kaden, *Helv. Chim. Acta*, 1989, **72**, 131; D. G. Fortier and A. McAuley, *Inorg. Chem.*, 1989, **28**, 655; J. Kim, M. P. Suh and W. Shin, *Acta Crystallogr., Sect. C*, 1991, **47**, 745; K. A. Beveridge, A. McAuley and C. Xu, *Inorg. Chem.*, 1991, **30**, 2074; A. McAuley, S. Subramanian and M. J. Zaworotko, *J. Chem. Soc., Chem. Commun.*, 1992, 1321; R. Edwards, P. D. Newman, F. S. Stephens, R. S. Vagg and P. A. Williams, *Inorg. Chim. Acta*, 1993, **204**, 125; J. M. Harrowfield, A. M. Sargeson, B. W. Skelton and A. H. White, *Aust. J. Chem.*, 1994, **47**, 181.
3 M. J. D'Aniello, jun., M. T. Mocella, F. Wagner, E. K. Barefield and I. C. Paul, *J. Am. Chem. Soc.*, 1975, **97**, 192; S. F. Lincoln, T. W. Hambley, D. L. Pisaniello and J. H. Coates, *Aust. J. Chem.*, 1984, **37**, 713; M. Kato and T. Ito, *Bull. Chem. Soc. Jpn.*, 1986, **59**, 285; M. S. Ram, C. G. Riordan, R. Ostrander and A. L. Rheingold, *Inorg. Chem.*, 1995, **34**, 5884.
4 N. W. Alcock, A. C. Benniston, S. J. Grant, H. A. A. Omar and P. Moore, *J. Chem. Soc., Chem. Commun.*, 1991, 1573.
5 E. Kimura, M. Haruta, T. Koike, M. Shionoya, K. Takenouchi and Y. Iitaaka, *Inorg. Chem.*, 1993, **32**, 2779.
6 S. Crick, R. W. Gable, B. F. Hoskins and P. A. Tregloan, *Inorg. Chim. Acta*, 1986, **111**, 35.
7 T. W. Hambley, *J. Chem. Soc., Dalton Trans.*, 1986, 565.
8 T. Ito, H. Ito and K. Toriumi, *Acta Crystallogr., Sect. B*, 1981, **37**, 1412.
9 E. Kimura, S. Wada, M. Shionoya, T. Takahashi and Y. Iitaka, *J. Chem. Soc., Chem. Commun.*, 1990, 397.
10 R. D. Hancock, M. P. Ngwenya, P. W. Wade, J. A. Boeyens and S. M. Dobson, *Inorg. Chim. Acta*, 1989, **164**, 73.
11 K. Kobiro, A. Nakayama, T. Hiro, M. Suma and Y. Tobe, *Inorg. Chem.*, 1992, **31**, 676.
12 M. P. Suh, S. G. Kang, V. L. Goedken and S. H. Park, *Inorg. Chem.*, 1991, **30**, 365.
13 D. D. Perrin and W. L. F. Armarego, *Purification of Laboratory Chemicals*, 3rd edn., Pergamon, Oxford, 1988.
14 G. M. Sheldrick, SHELXS 86, Program for the Solution of Crystal Structures, University of Göttingen, 1986.
15 G. M. Sheldrick, SHELXL 93, Program for the Refinement of Crystal Structures, University of Göttingen, 1993.
16 E. Iwamoto, T. Yokoyama, S. Yamasaki, T. Yabe, T. Kumamaru and Y. Yamamoto, *J. Chem. Soc., Dalton Trans.*, 1988, 1935.
17 T. Ito, H. Ito and K. Toriumi, *Chem. Lett.*, 1981, 1101.
18 (*a*) B.-F. Liang and C.-S. Chung, *Inorg. Chem.*, 1981, **20**, 2152; (*b*) E. J. Billo, *Inorg. Chem.*, 1984, **23**, 236; (*c*) J.-W. Chen, D.-S. Wu and C.-S. Chung, *Inorg. Chem.*, 1986, **25**, 1940.
19 E. K. Barefield, G. M. Freeman and D. G. Van Derveer, *Inorg. Chem.*, 1986, **25**, 552.
20 M. P. Suh, H. K. Kim, M. Kim and K. Y. Oh, *Inorg. Chem.*, 1992, **31**, 3620; E. K. Barefield, G. M. Freeman and D. G. Van Derveer, *Inorg. Chem.*, 1986, **25**, 552; G. Goloub, H. Cohen and D. Meyerstein, *J. Chem. Soc., Chem. Commun.*, 1992, 397; G. Goloub, H. Cohen, P. Paoletti, A. Bencini, L. Messori, I. Bertini and D. Meyerstein, *J. Am. Chem. Soc.*, 1995, **117**, 8385.
21 C. K. Johnson, ORTEP, Report ORNL-5138. Oak Ridge National Laboratory, Oak Ridge, TN, 1976.
22 F. Wagner and E. K. Barefield, *Inorg. Chem.*, 1976, **15**, 408; F. Wagner, M. T. Mocella, M. J. D'Aniello, jun., A. H. J. Wang and E. K. Barefield, *J. Am. Chem. Soc.*, 1974, **96**, 2625; B. Bosnich, R. Mason, P. J. Pauling, G. B. Robertson and M. L. Tobe, *Chem. Commun.*, 1965, 97; N. J. Jubran, G. Zinzburg, H. Cohen, Y. Koresh and D. Meyerstein, *Inorg. Chem.*, 1985, **24**, 251.
23 M. P. Suh, B. Y. Shim and T.-S. Yoon, *Inorg. Chem.*, 1994, **33**, 5509.
24 B.-F. Liang, D. W. Margerum and C.-S. Chung, *Inorg. Chem.*, 1979, **18**, 2001; B.-F. Liang and C.-S. Chung, *Inorg. Chem.*, 1980, **19**, 1867.
25 O. Barton and W. D. Ollis, *Comprehensive Organic Chemistry*, Pergamon, Oxford, 1979, vol. 2, p. 83.
26 M. P. Suh, W. Shin, H. Kim and C. H. Koo, *Inorg. Chem.*, 1987, **26**, 1846.

27 M. P. Suh, W. Shin, S. G. Kang, M. S. Lah and T. M. Chung, *Inorg. Chem.*, 1989, **28**, 1602.
28 C.-C. Chang and C.-S. Chung, *J. Chem. Soc., Dalton Trans.*, 1991, 883.
29 F. Basolo and R. G. Pearson, *Mechanisms of Inorgaic Reactions*, 2nd edn., Wiley, New York, 1962; D. W. Barnum, *Inorg. Chem.*, 1983, **22**, 2297; J. Suh, B. K. Hwang and Y. H. Koh, *Bioorg. Chem.*, 1990, **18**, 207; J. Suh, *Bioorg. Chem.*, 1990, **18**, 345; J. Suh, T. H. Park and B. K. Hwang, *J. Am. Chem. Soc.*, 1991, **113**, 883; J. Suh, *Acc. Chem. Res.*, 1992, **25**, 273.
30 R. A. Read and D. W. Margerum, *Inorg. Chem.*, 1981, **20**, 3143 and refs. therein.
31 P. Moore, J. Sachinidis and G. R. Willey, *J. Chem. Soc., Chem. Commun.*, 1983, 522.
32 S. F. Lincoln, D. L. Pisaniello, J. H. Coates and D. A. Hadi, *Inorg. Chim. Acta*, 1984, **81**, L9.
33 J. R. Röper and H. Elias, *Inorg. Chem.*, 1992, **31**, 1202.
34 P. O. Whimp, M. F. Bailey and N. F. Curtis, *J. Chem. Soc. A*, 1970, 1956.
35 M. P. Suh, K. Y. Oh, J. W. Lee and Y. Y. Bae, *J. Am. Chem. Soc.*, 1996, **118**, 777.

Received 26*th July* 1996*; Paper* 6/05255J